遠地津波に関する時間遅れと初動反転の原因と対策

綿田辰吾(東京大学地震研究所)

- Tsunami observation Deep-ocean Assessment Reports of Tsunamis (DART) buoys

DART Mooring System

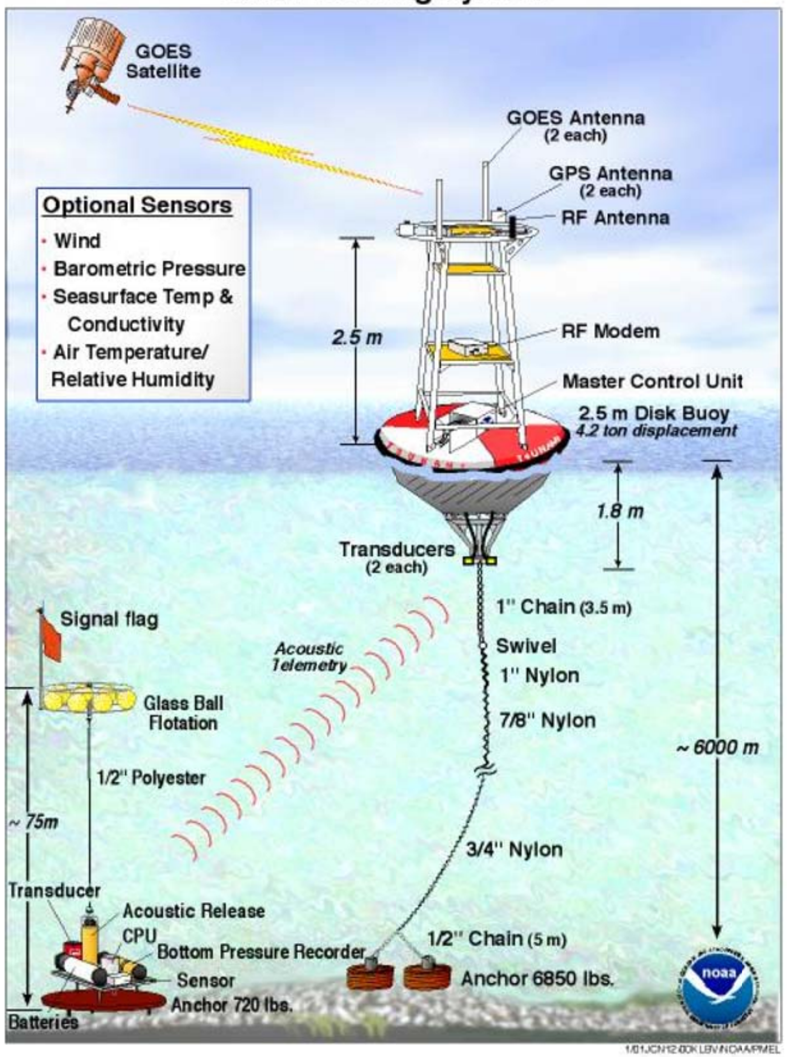

- DART buoys in the Pacific
  - To avoid
    interference of coastal reflection
    non-linear effects at shallow oceans

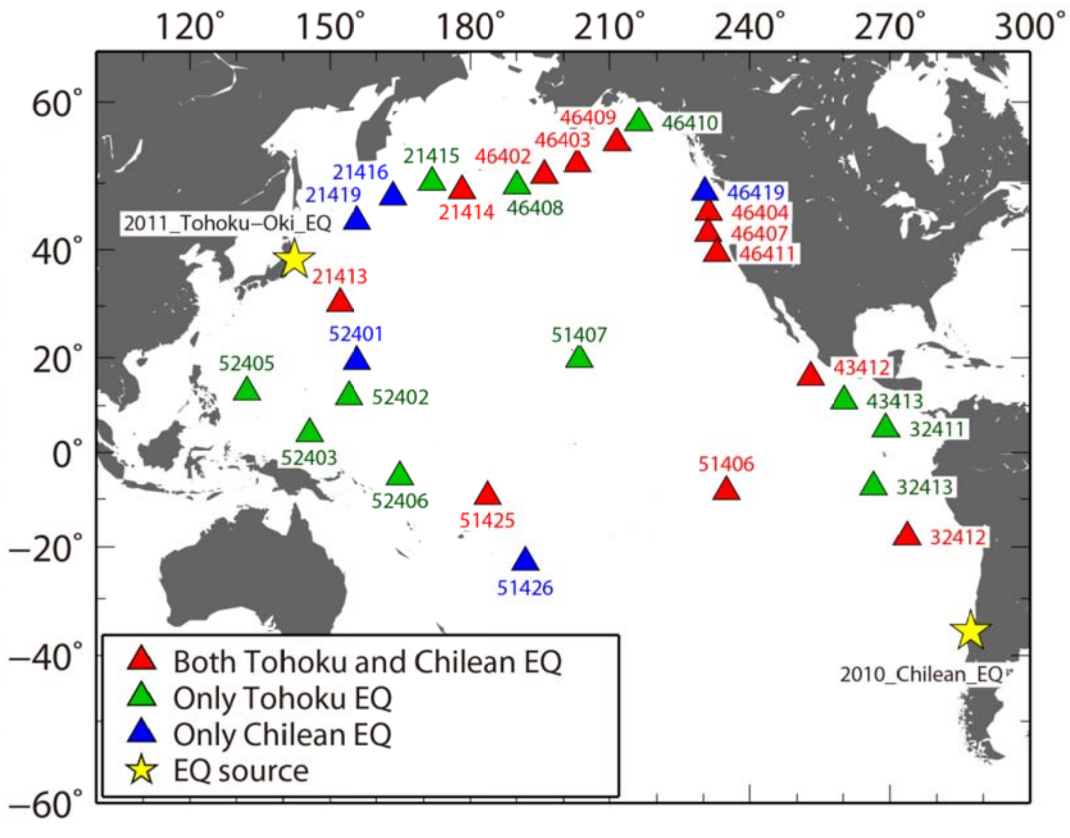

2010 Chilean EQ tsunami

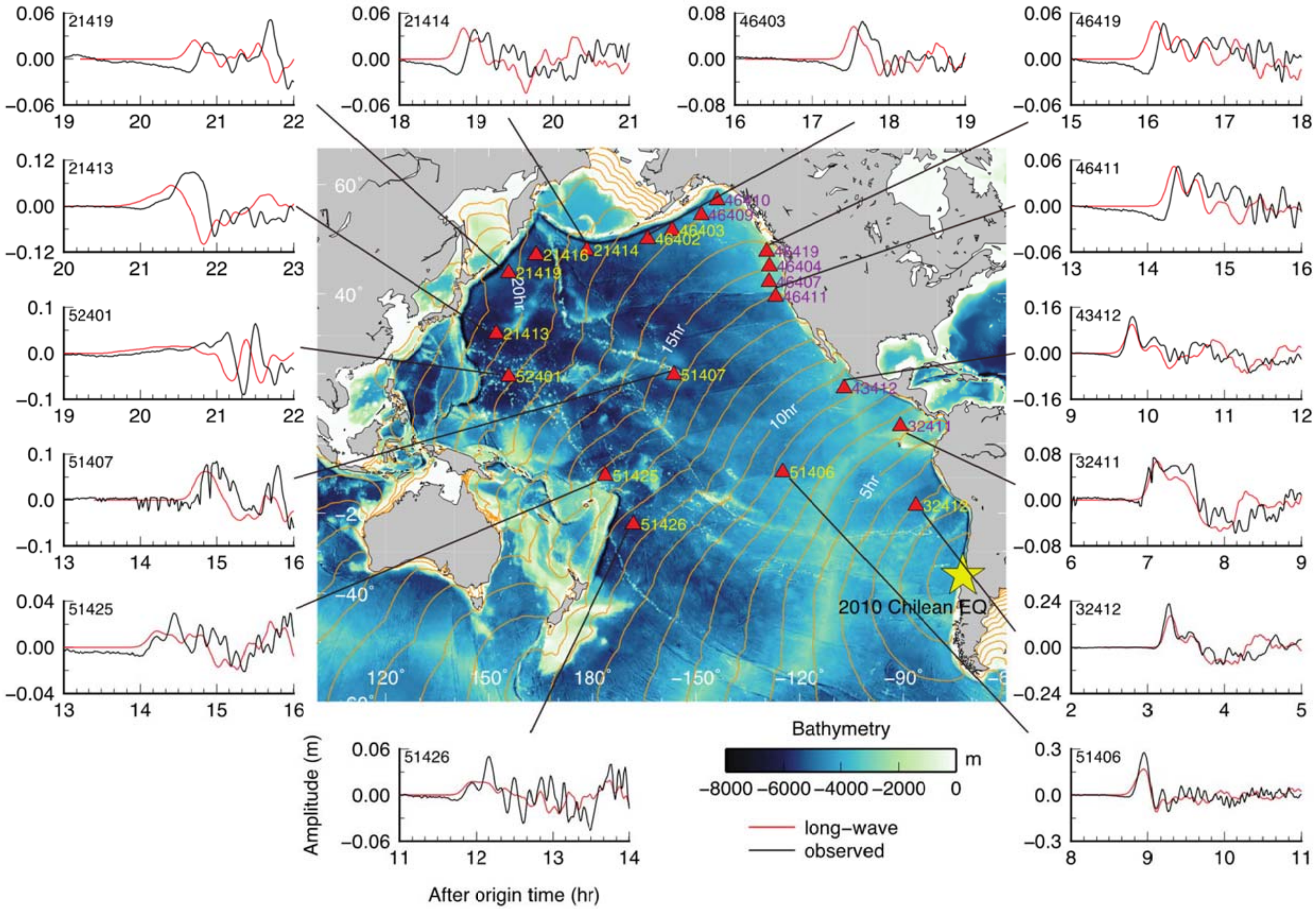

2011 Tohoku-Oki EQ tsunami

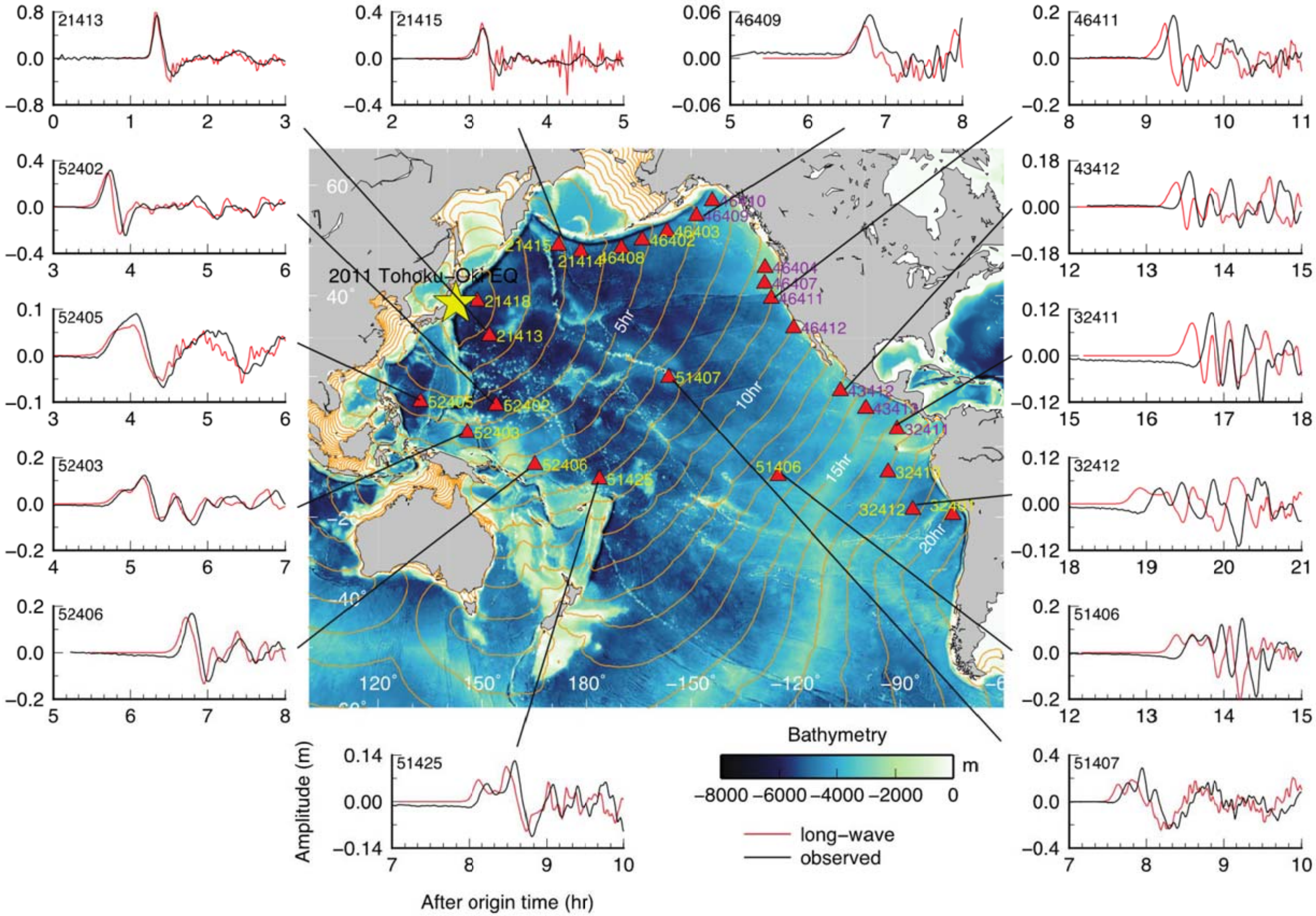

Traveltime anomalies from 2010 Chile and 2011 Tohoku-Oki EQ tsunamis.
Small initial negative phases at distant locations.

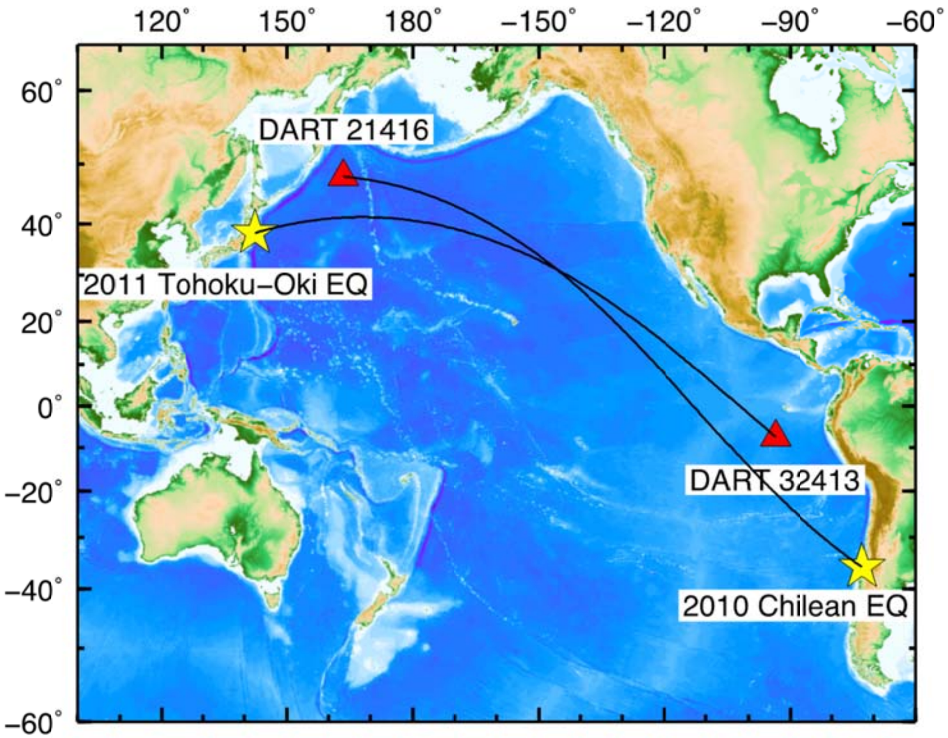

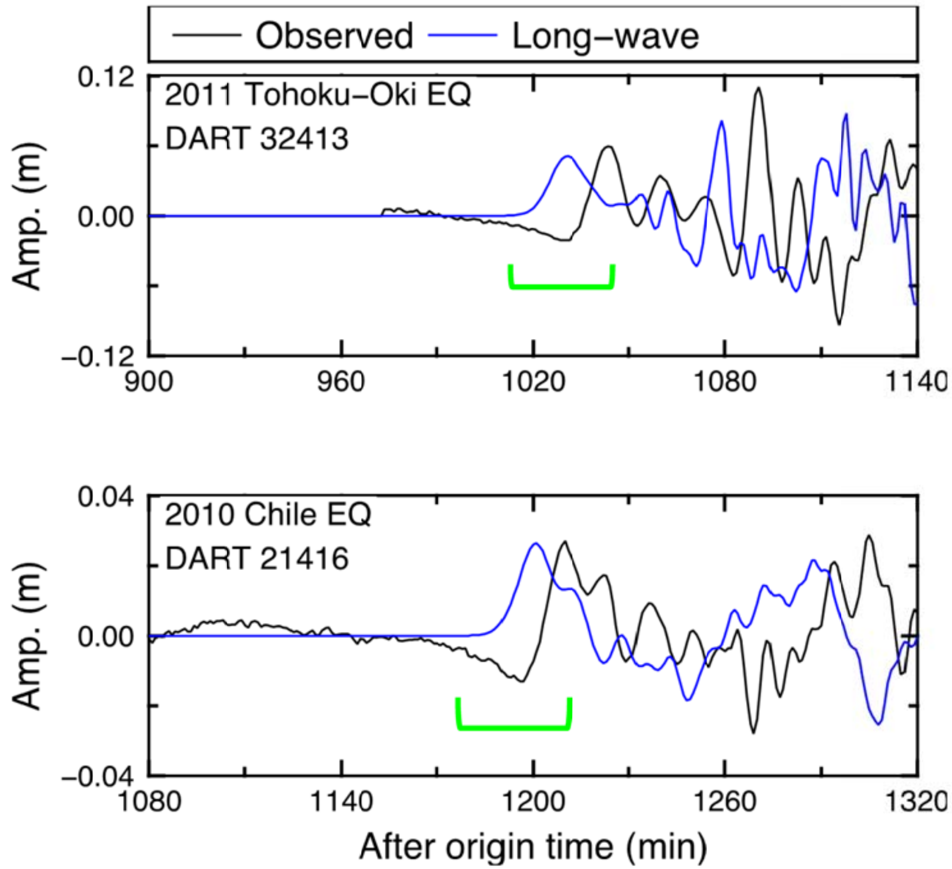

$$\frac{\Delta c(tsunami)}{c(tsunami)} \approx \textbf{-1.2\%}$$

Observed traveltime – Long-wave simulation traveltime

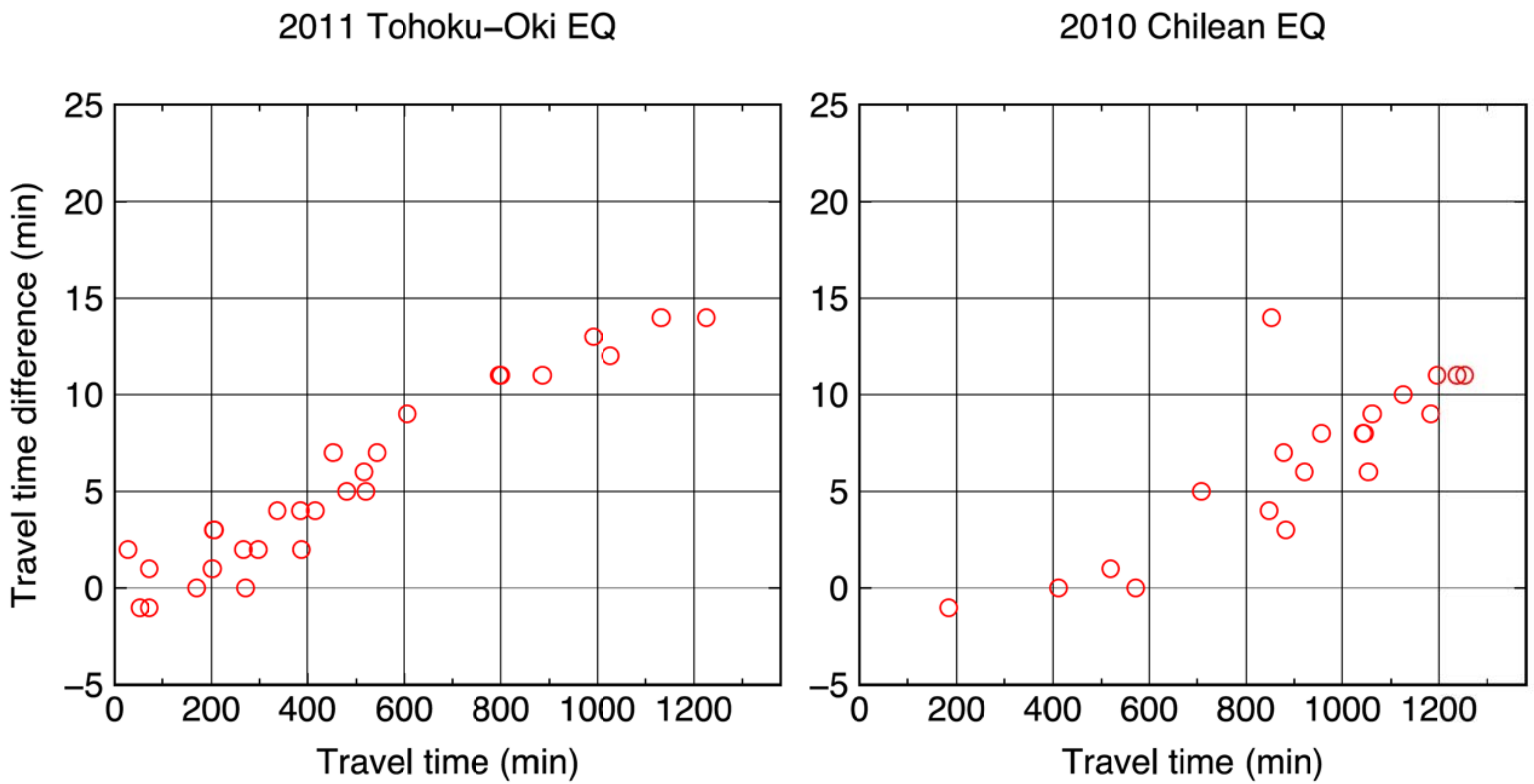

$$\frac{\Delta c(tsunami)}{c(tsunami)} \approx \textbf{-1.2\%}$$

2011 Tohoku earthquake

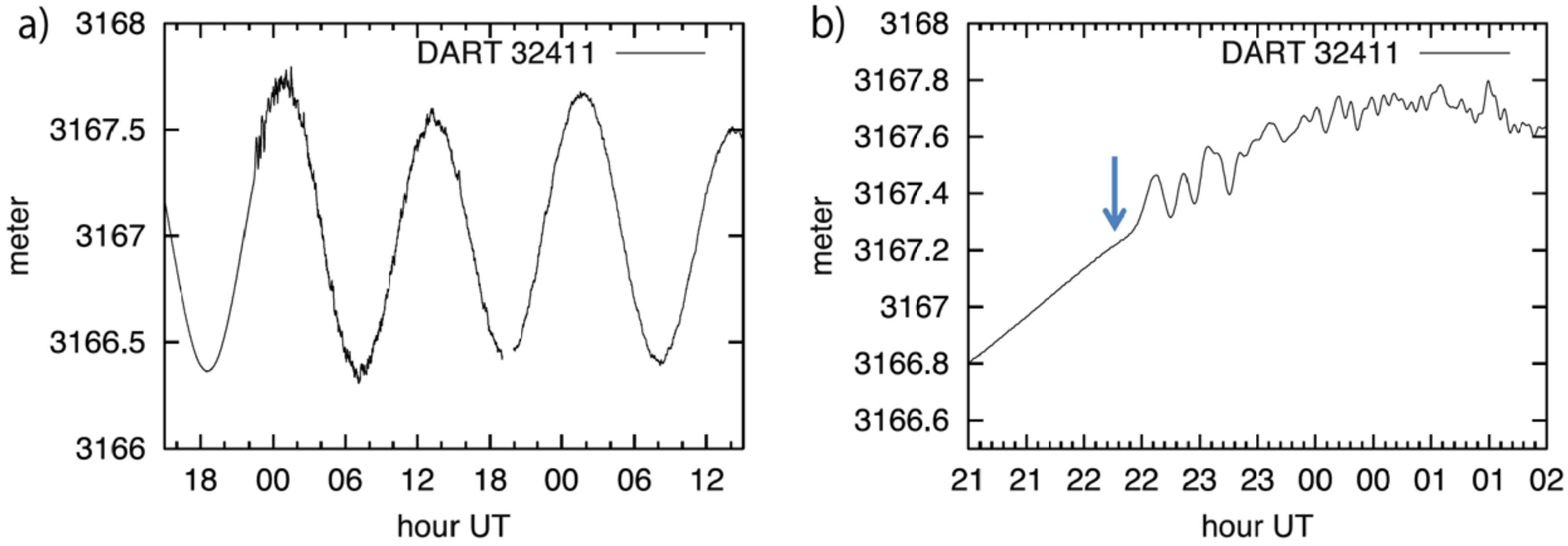

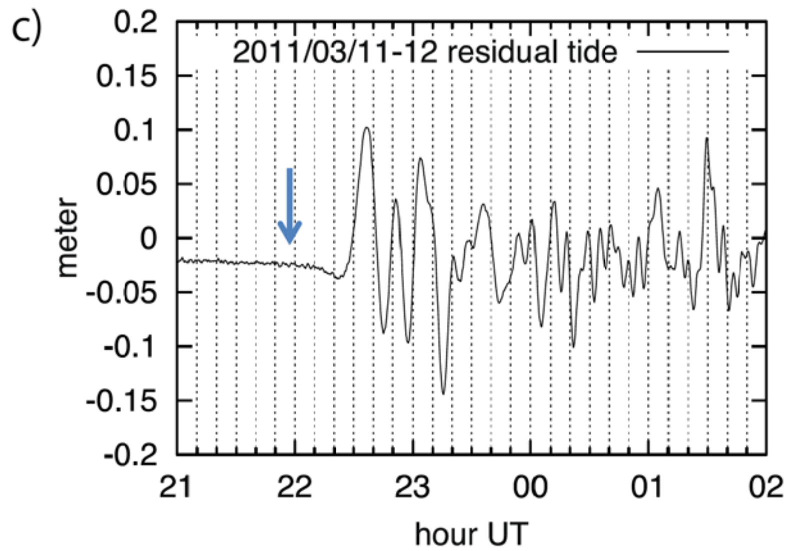

De-tided records show a initial phase with a negative polarity of the main peak.

2011 Tohoku-Oki EQ tsunami

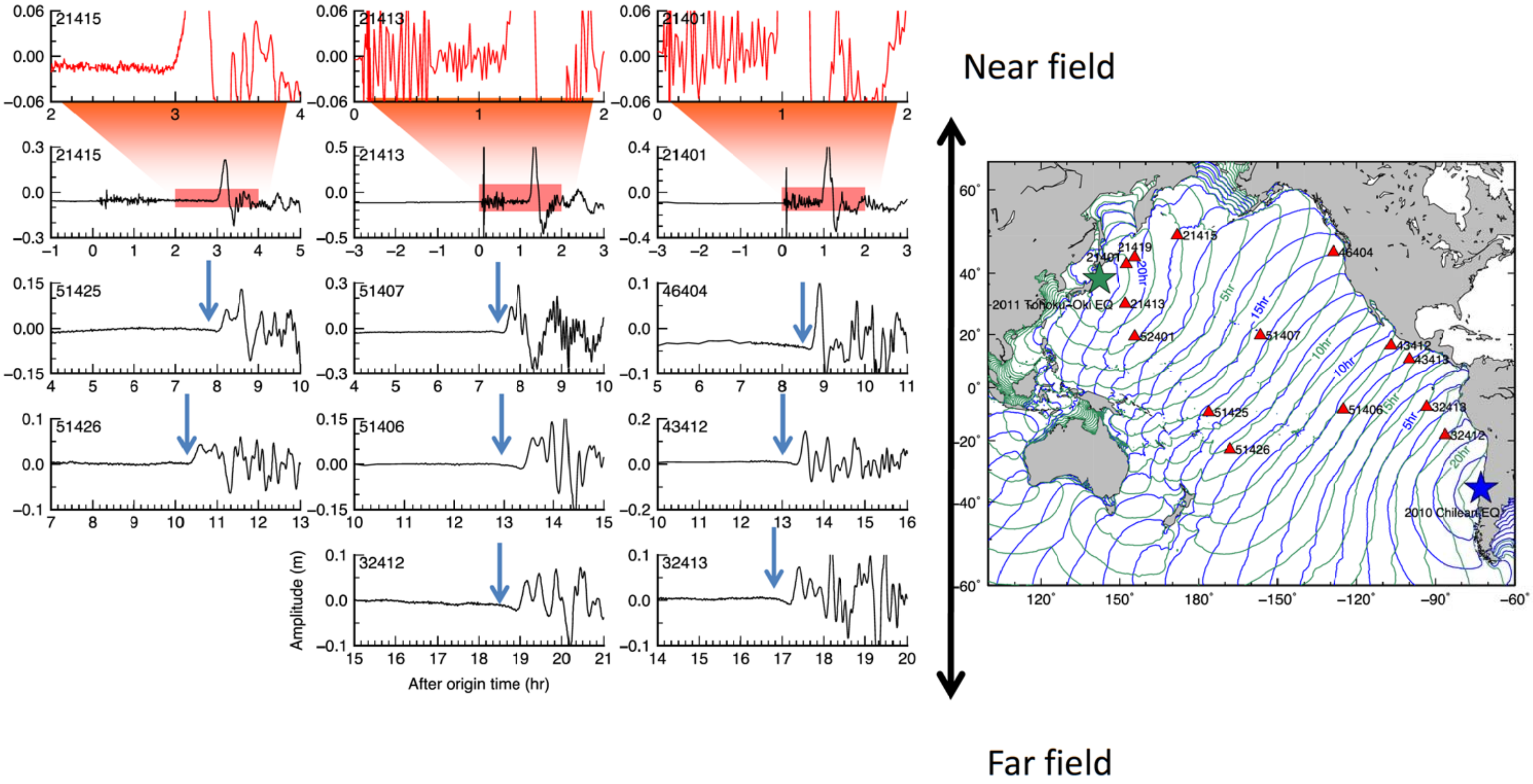

2010 Chilean EQ tsunami

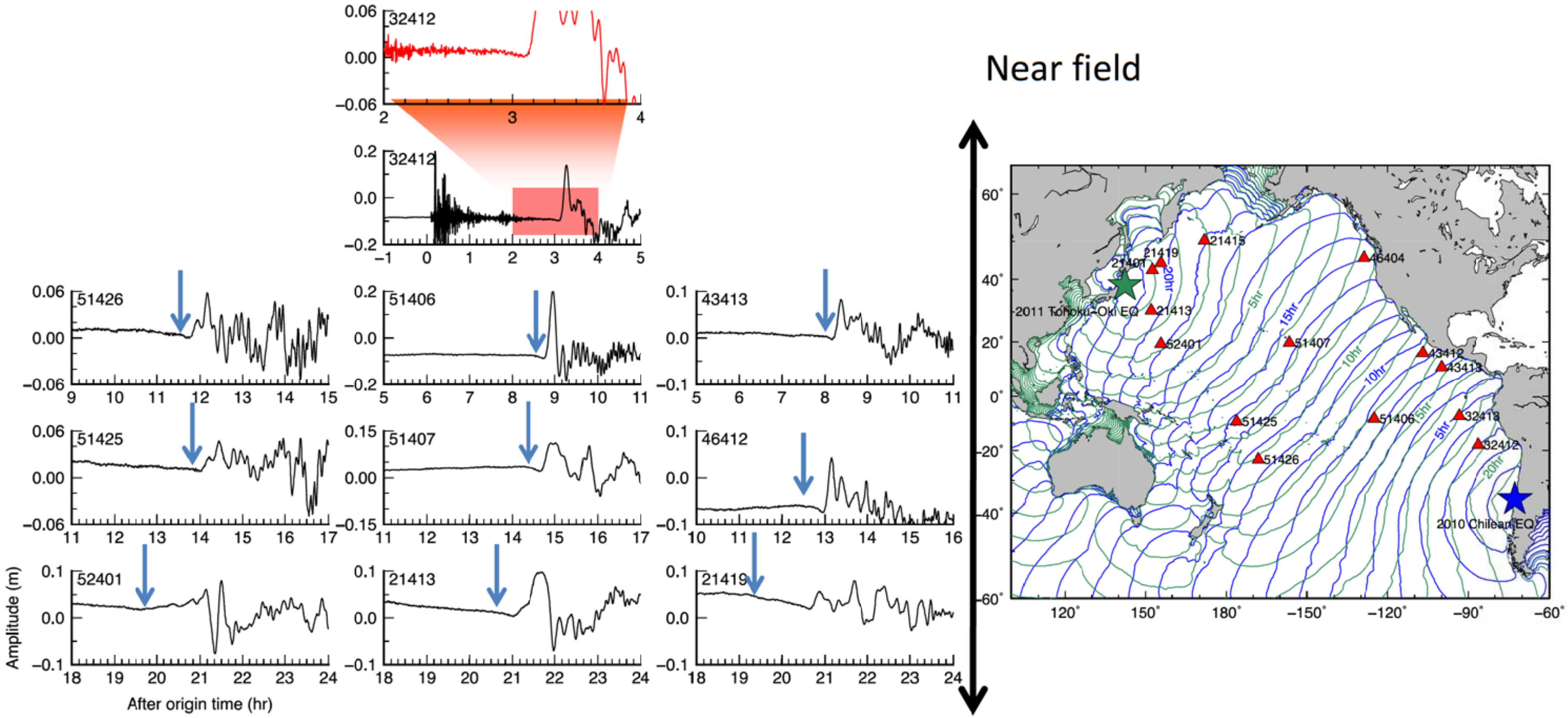

Near field

Far field

1. Time-variable gravity potential
2. Compressible water
3. Elastic earth

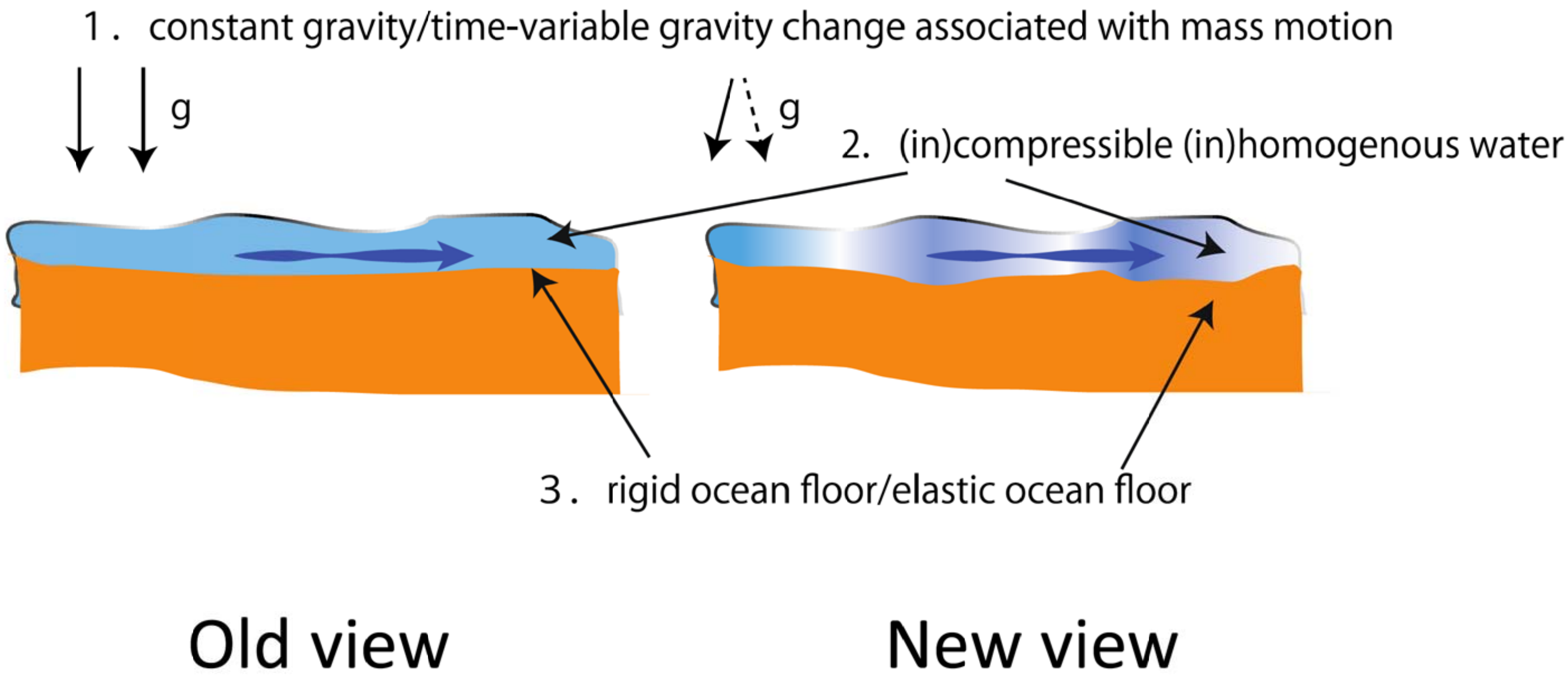

Tsunami propagation over 2D bathymetry of the real Earth

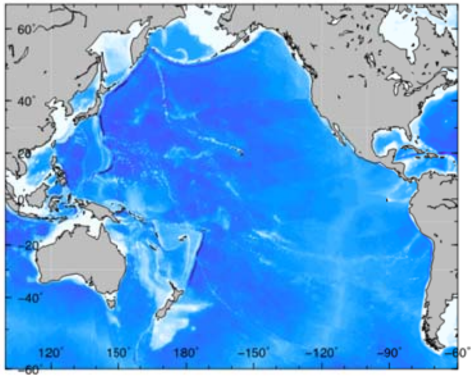

Locally 1D tsunami propagation coupled with the self-gravitating elastic Earth

1D Earth normal mode for PREM with an ocean layer

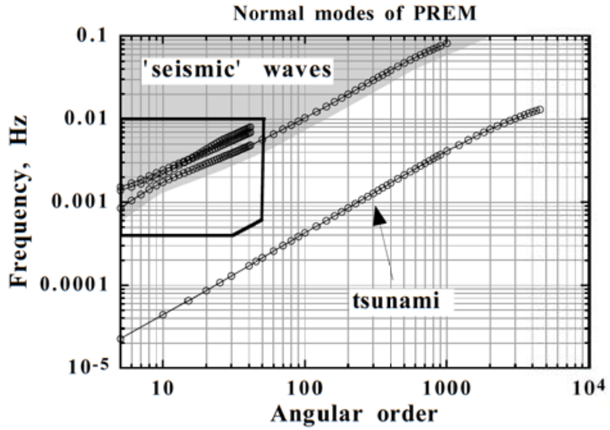

Fluid Part

from the linearized Navier-Stokes equation

$$\rho\frac{D^2\mathbf{u}}{Dt^2} = -\nabla P + \rho\mathbf{g}.$$

Equation of continuity

$$\delta\rho + \rho\nabla\cdot\mathbf{u} = 0.$$

The adiabatic equation of state for an ideal fluid

$$\delta\rho = \left(\frac{\partial\rho}{\partial P}\right)_S \delta P = \frac{\delta P}{c^2}.$$

The Poisson equation for gravitational potential

$$\nabla^2\phi = 4\pi\rho.$$

The definition of the gravitational potential

$$\mathbf{g} = -\nabla\phi.$$

\+

Solid Part

Momentum eq.

……

Equation of cont.

….

Constitutive eq.

…

Poisson eq. for gravity pot.

….

Definition of gravity

….

\+ Boundary Condition

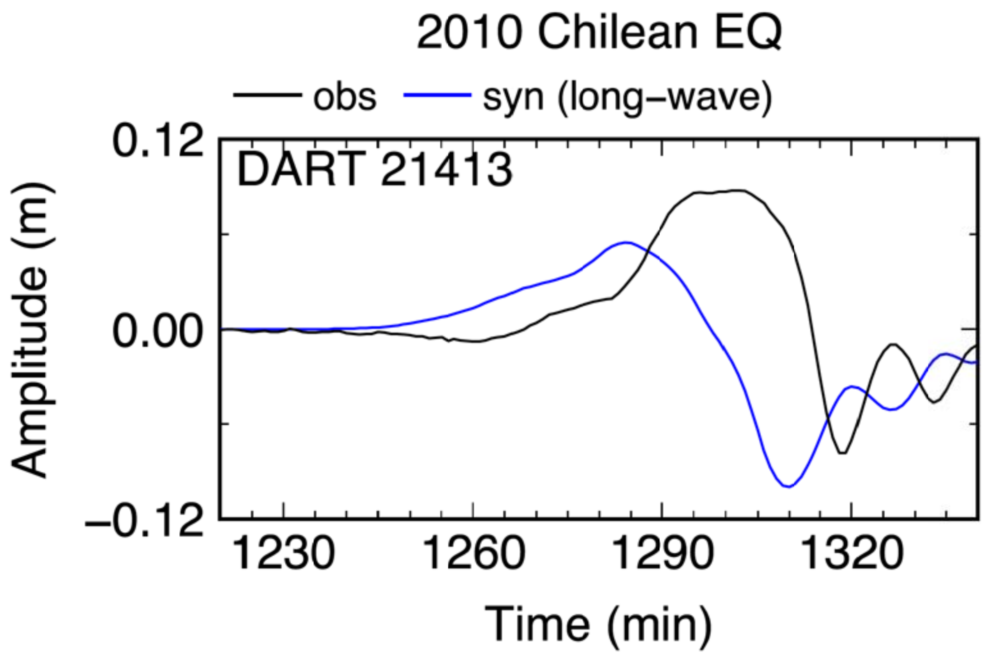

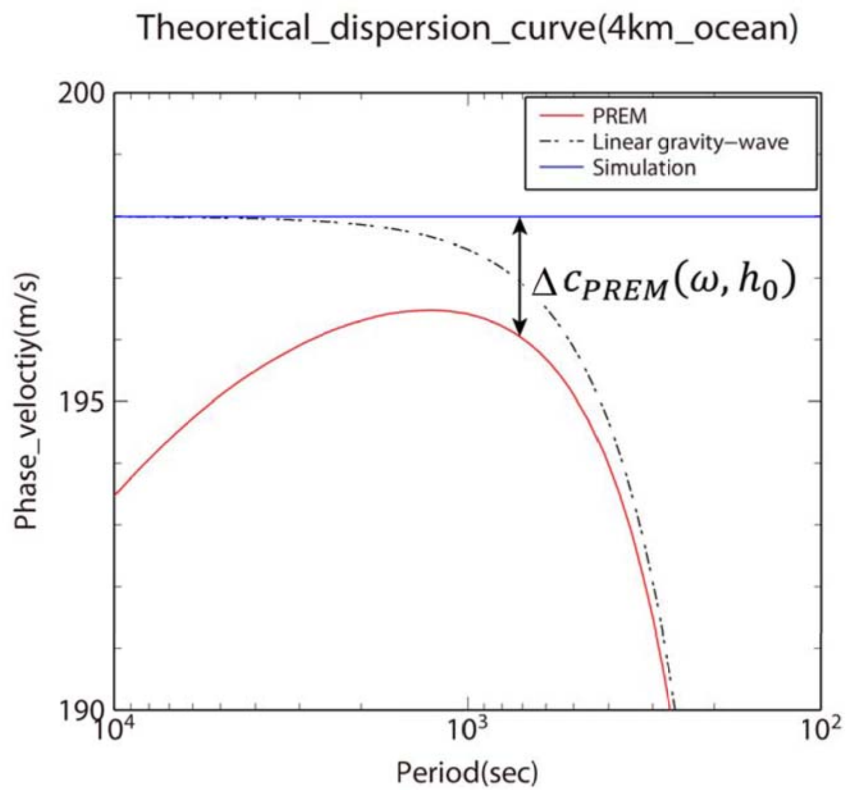

$$u(x,t) = \frac{1}{\pi}\int_0^\infty \hat{u}(x,\omega)\cos(\Psi(x,\omega))d\omega$$

$\Psi(x,\omega)$: Phase spectrum

Phase difference between observation and long-wave simulation

$$\Delta\Psi(x,\omega) = \int_0^x \Delta\Psi(dx,\omega)\,dx = \int_0^x \frac{\Delta c(\omega,x)\omega}{gD(x)}dx$$

depth-normalized phase velocity difference

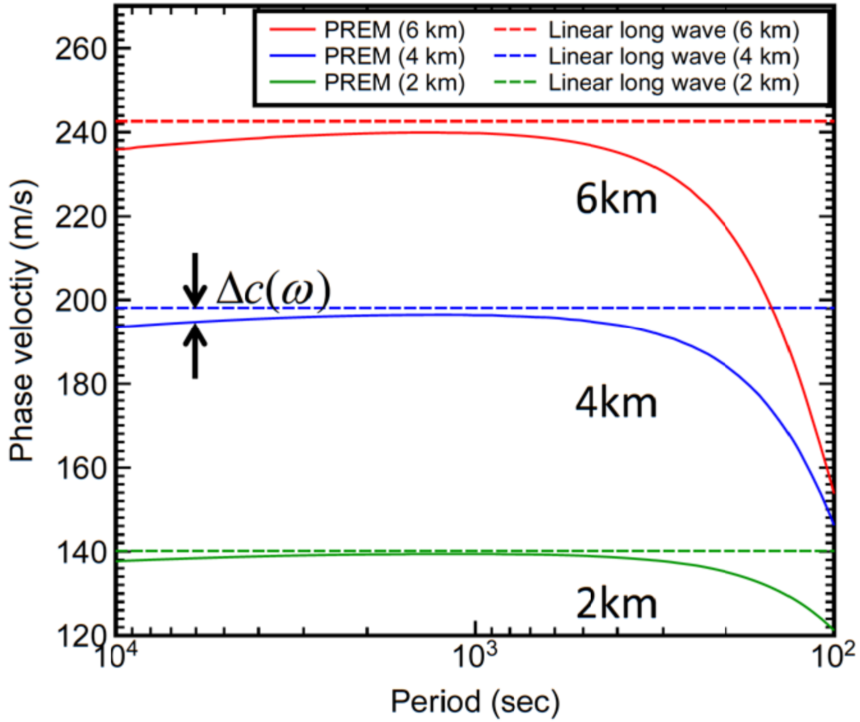

We found

$$\frac{\Delta c(\omega)}{D} = \frac{\Delta c_o(\omega)}{D_o},$$ For all linear long-waves

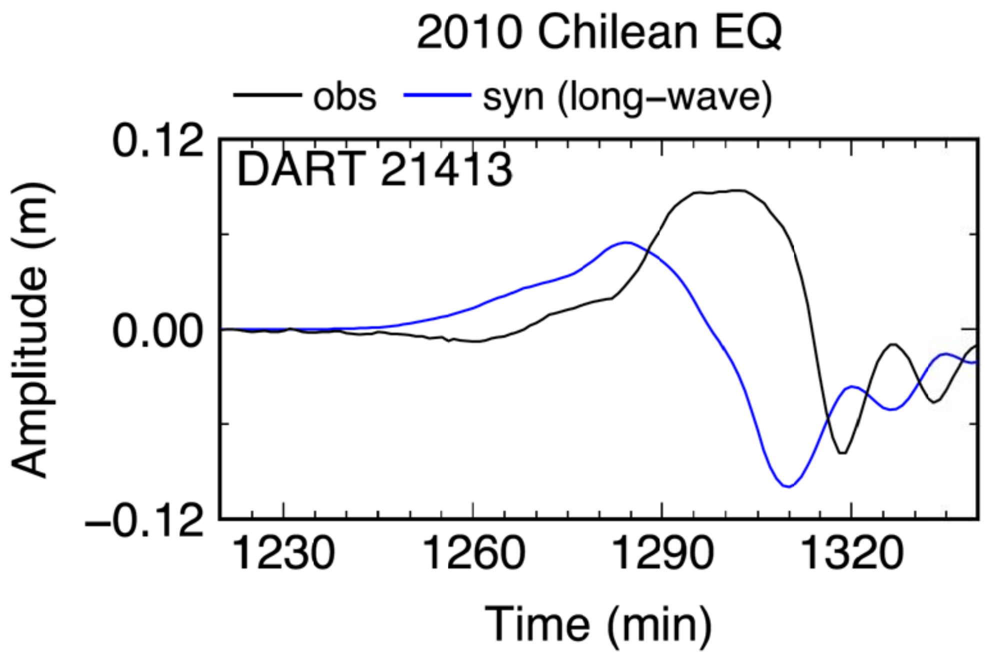

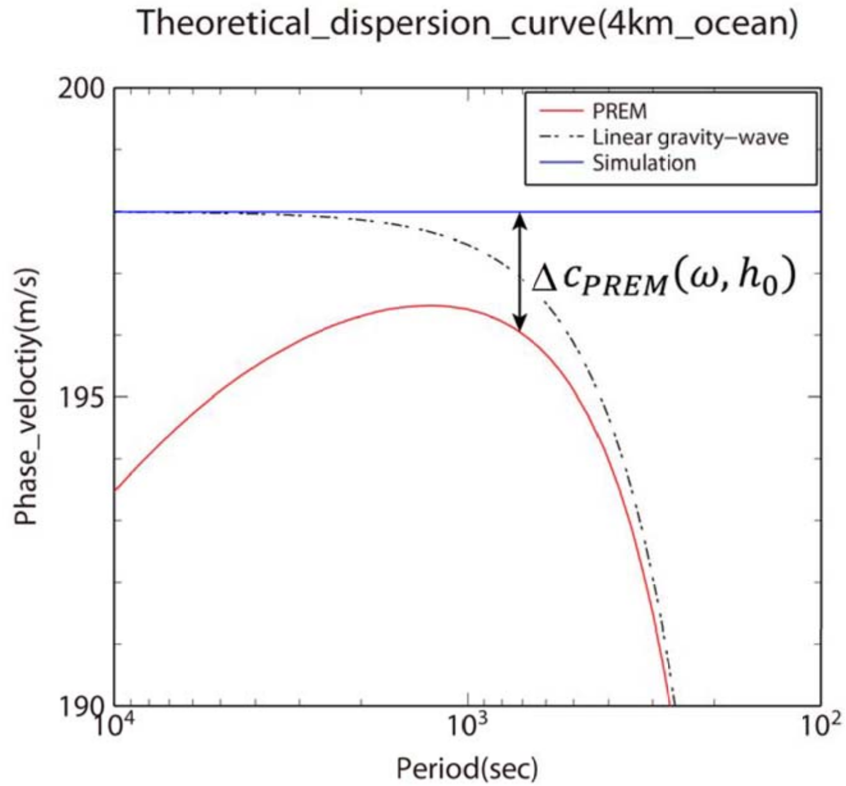

$$u(x,t) = \frac{1}{\pi}\int_0^{\infty} \hat{u}(x,\omega)\cos(\Psi(x,\omega))d\omega$$

$\Psi(x,\omega)$: Phase spectrum

Phase difference between observation and long-wave simulation

$$\Delta\Psi(x,\omega) = \int_0^x \Delta\Psi(dx,\omega)dx = \int_0^x \frac{\Delta c(\omega,x)\omega}{gD(x)}dx = \frac{\Delta c_o(\omega)\omega}{gD_o}\int_0^x dx = \frac{\Delta c_o(\omega)\omega}{gD_o}L$$

Independent of D(x)

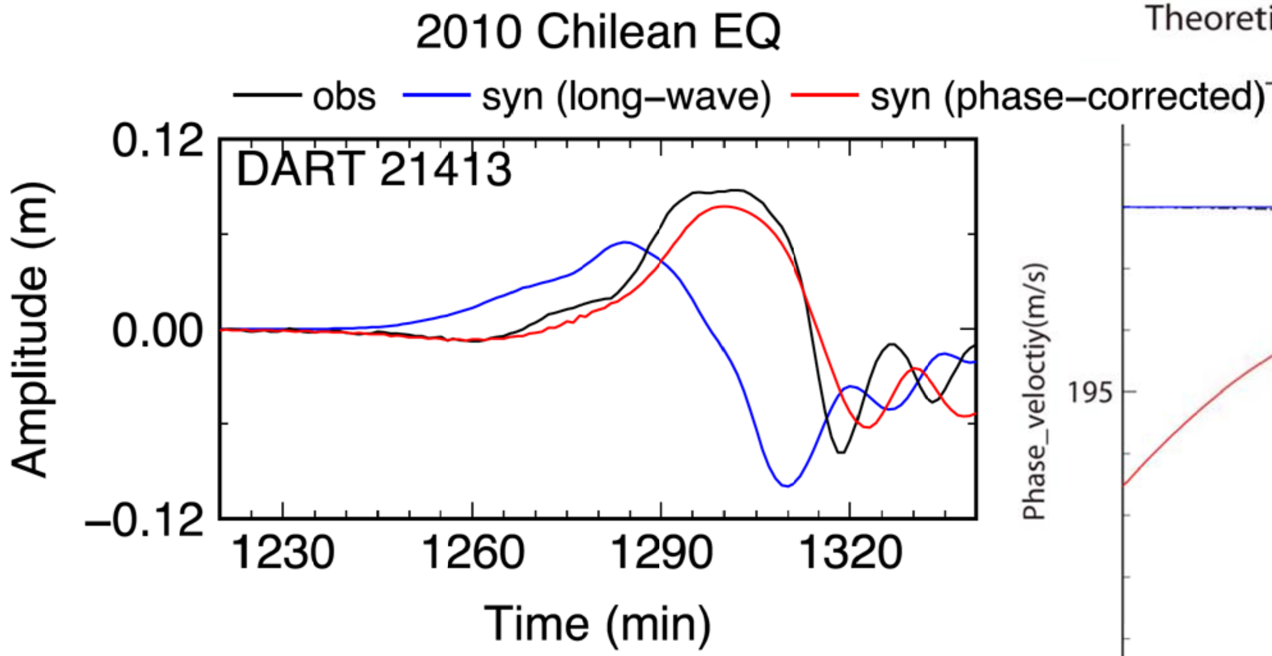

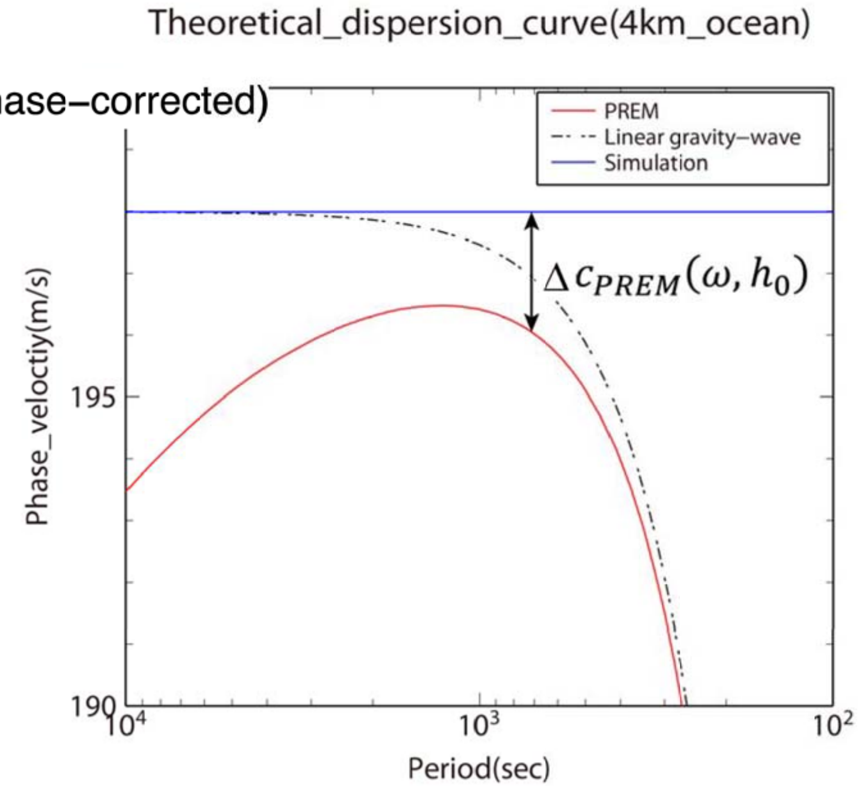

$$u(x,t) = \frac{1}{\pi}\int_0^\infty \hat{u}(x,\omega)\cos(\Psi(x,\omega))d\omega$$

$\Psi(x,\omega)$: Phase spectrum

Phase difference between observation and long-wave simulation

$$\Delta\Psi(x,\omega) = \int_0^x \Delta\Psi(dx,\omega)dx = \int_0^x \frac{\Delta c(\omega,x)\omega}{gD(x)}dx = \frac{\Delta c_o(\omega)\omega}{gD_o}\int_0^x dx = \frac{\Delta c_o(\omega)\omega}{gD_o}L$$

Independent of D(x)

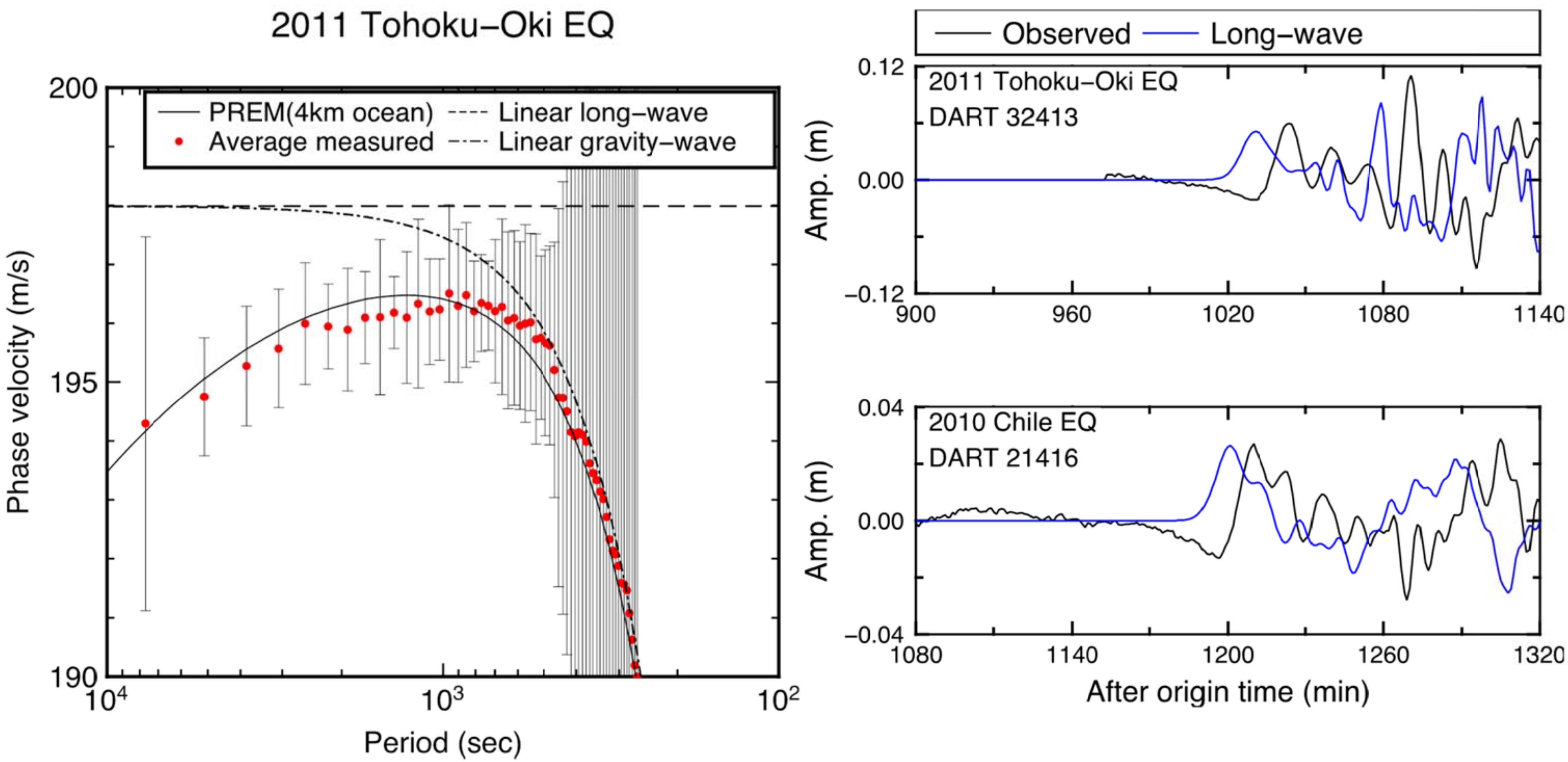

2011 Tohoku−Oki EQ
PREM(4km ocean)
Linear long−wave
Average measured
Linear gravity−wave
Phase velocity (m/s)
Period (sec)
200
195
190
10^4
10^3
10^2
Observed
Long−wave
2011 Tohoku−Oki EQ
DART 32413
Amp. (m)
0.12
0.00
−0.12
900
960
1020
1080
1140
2010 Chile EQ
DART 21416
0.04
0.00
−0.04
1080
1140
1200
1260
1320
After origin time (min)

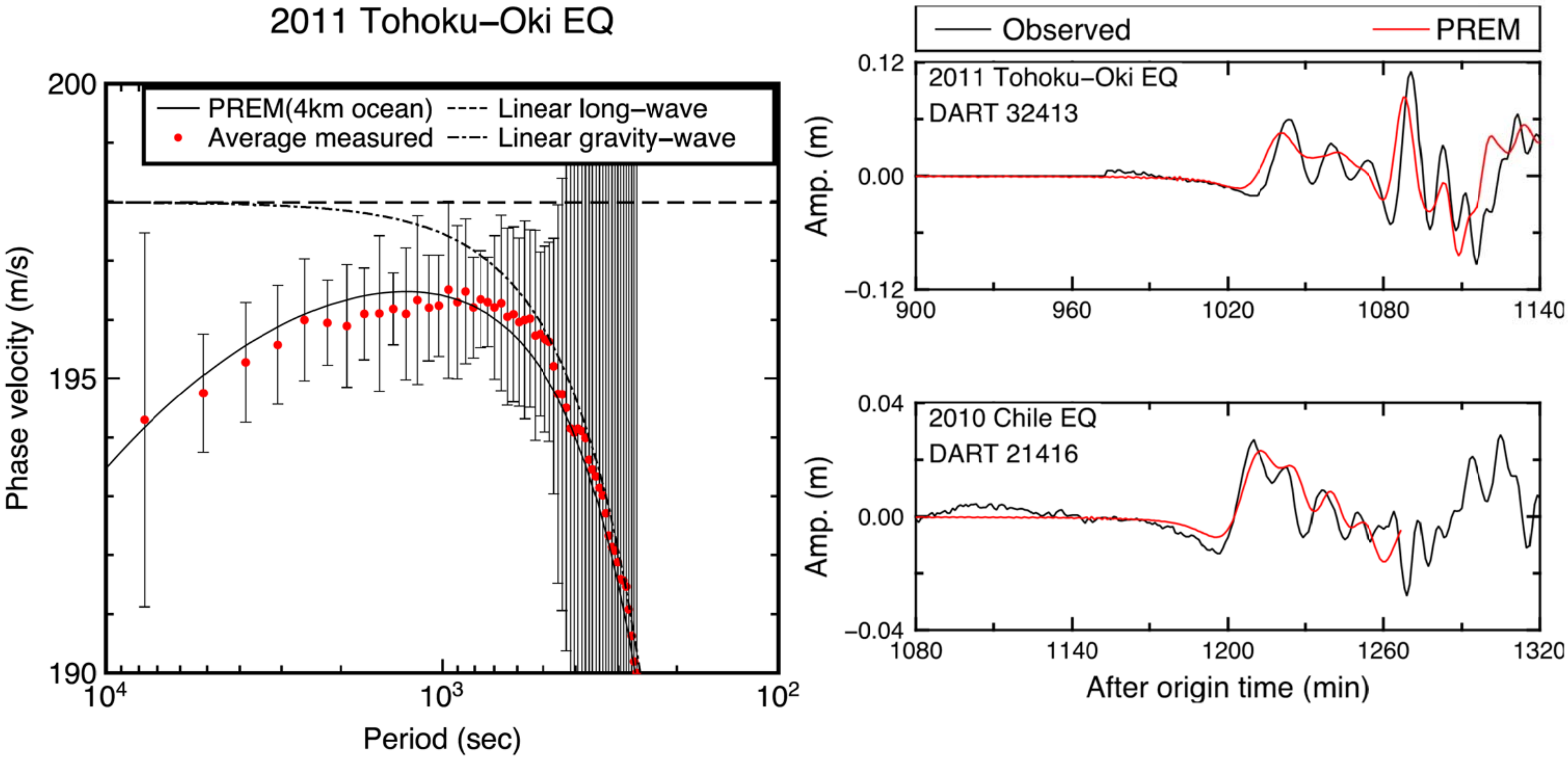

2011 Tohoku–Oki EQ
PREM(4km ocean)
Linear long–wave
Average measured
Linear gravity–wave
Phase velocity (m/s)
Period (sec)
Observed
PREM
2011 Tohoku–Oki EQ
DART 32413
2010 Chile EQ
DART 21416
Amp. (m)
After origin time (min)

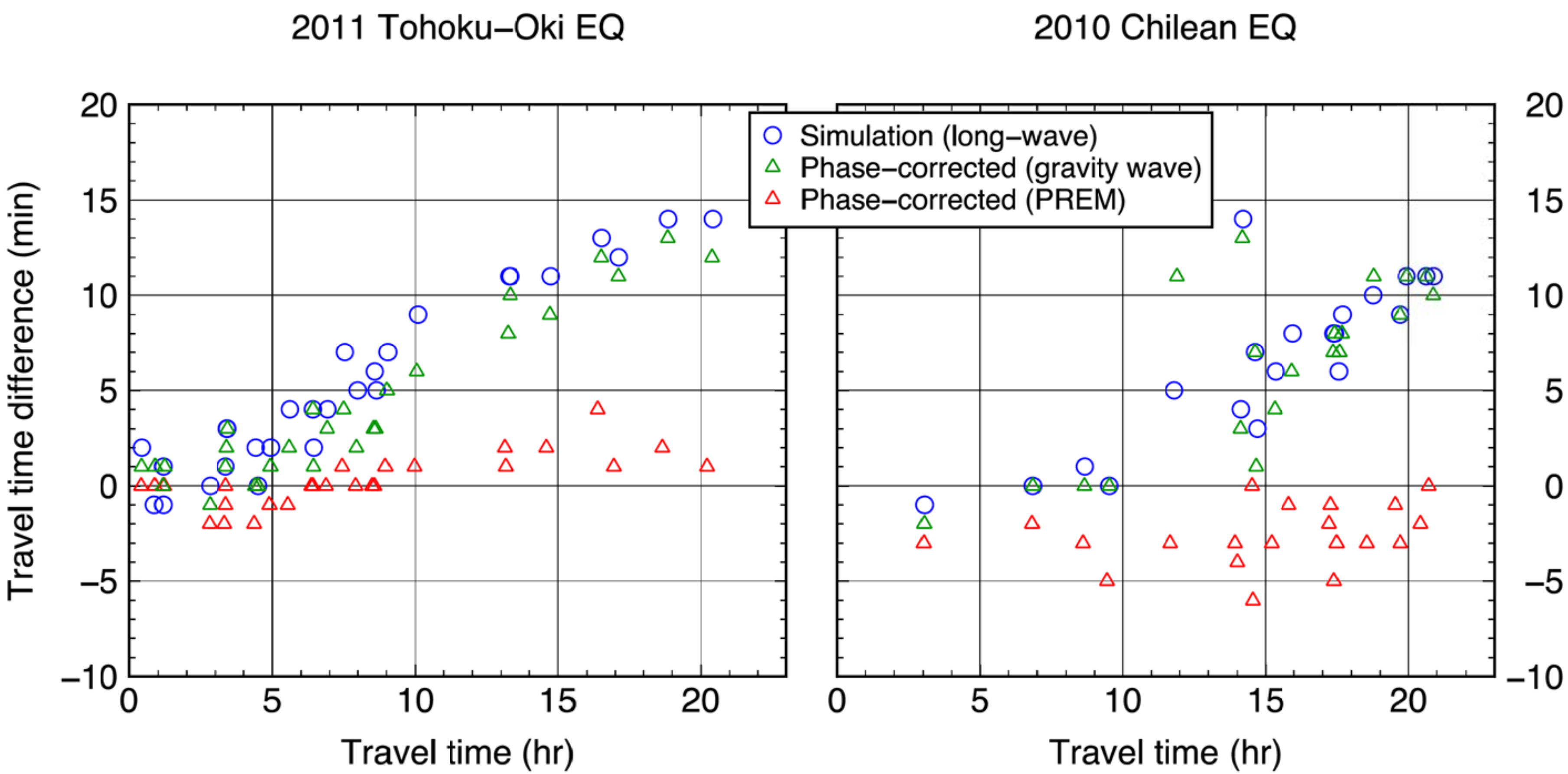

2011 Tohoku–Oki EQ
2010 Chilean EQ
Simulation (long–wave)
Phase–corrected (gravity wave)
Phase–corrected (PREM)
Travel time difference (min)
Travel time (hr)
Travel time (hr)
20
15
10
5
0
–5
–10
0
5
10
15
20

- **Seawater compressibility, elasticity of the solid Earth and gravity potential change are the main causes of the delay and small initial negative phase at distant tsunamis.**
- **A new economical method to compute synthetic tsunamis has been developed.**

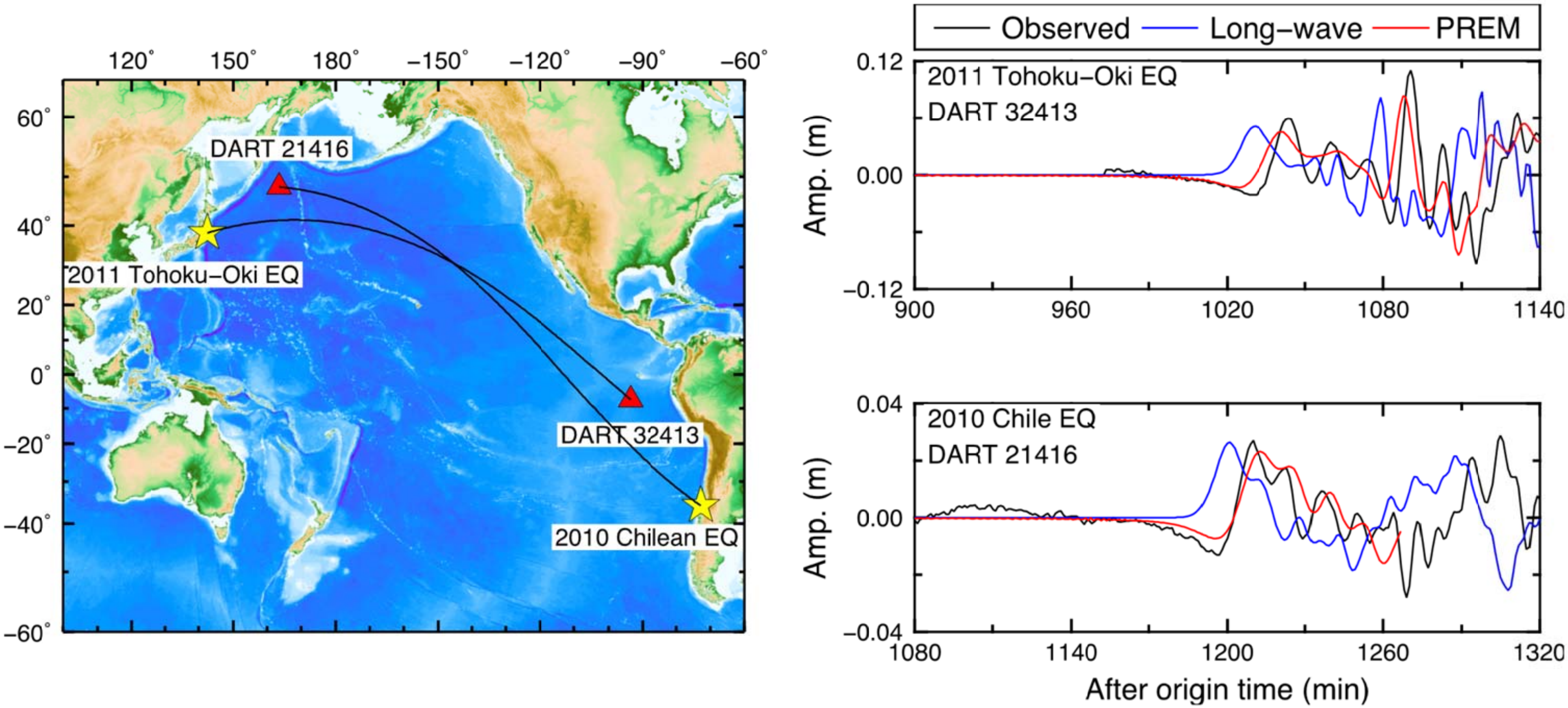

Contribution of compressible water, elastic Earth, gravitational potential change to tsunami phase velocity

Theoretical dispersion curve(4km ocean)

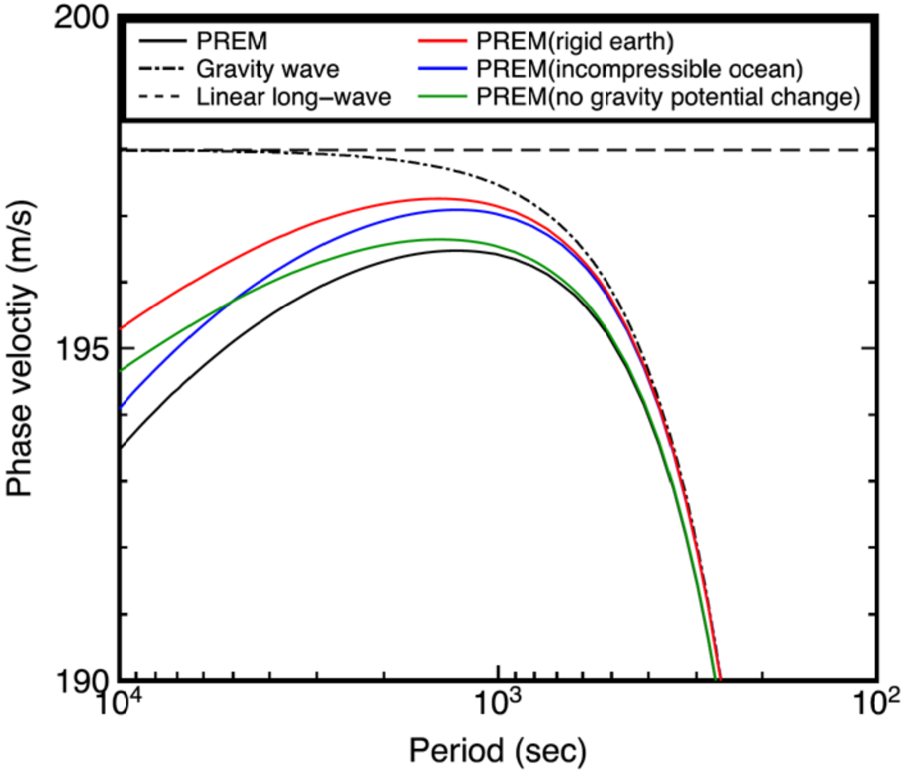

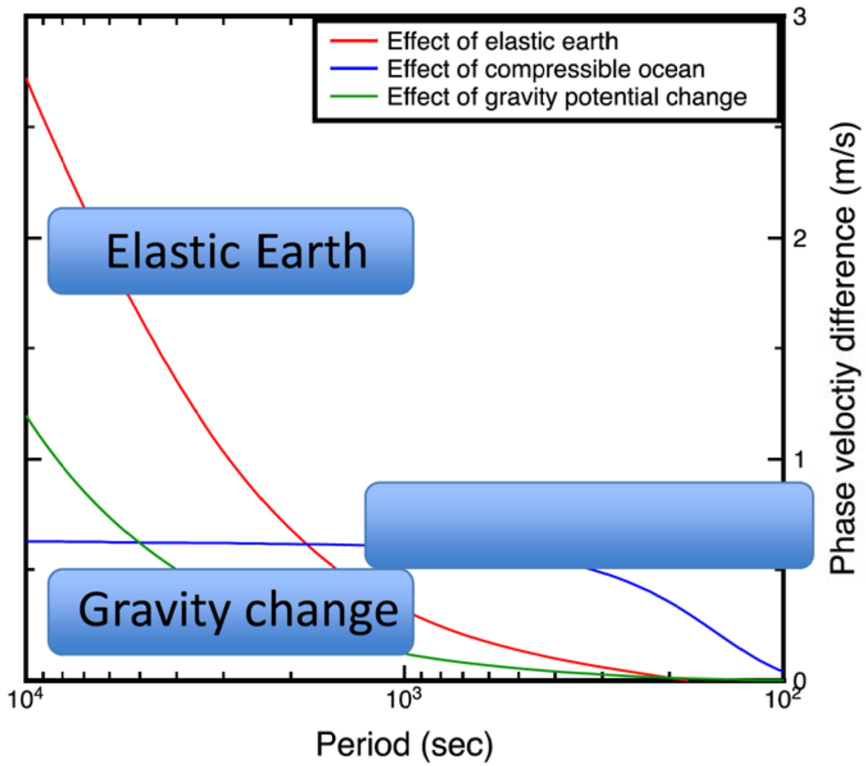

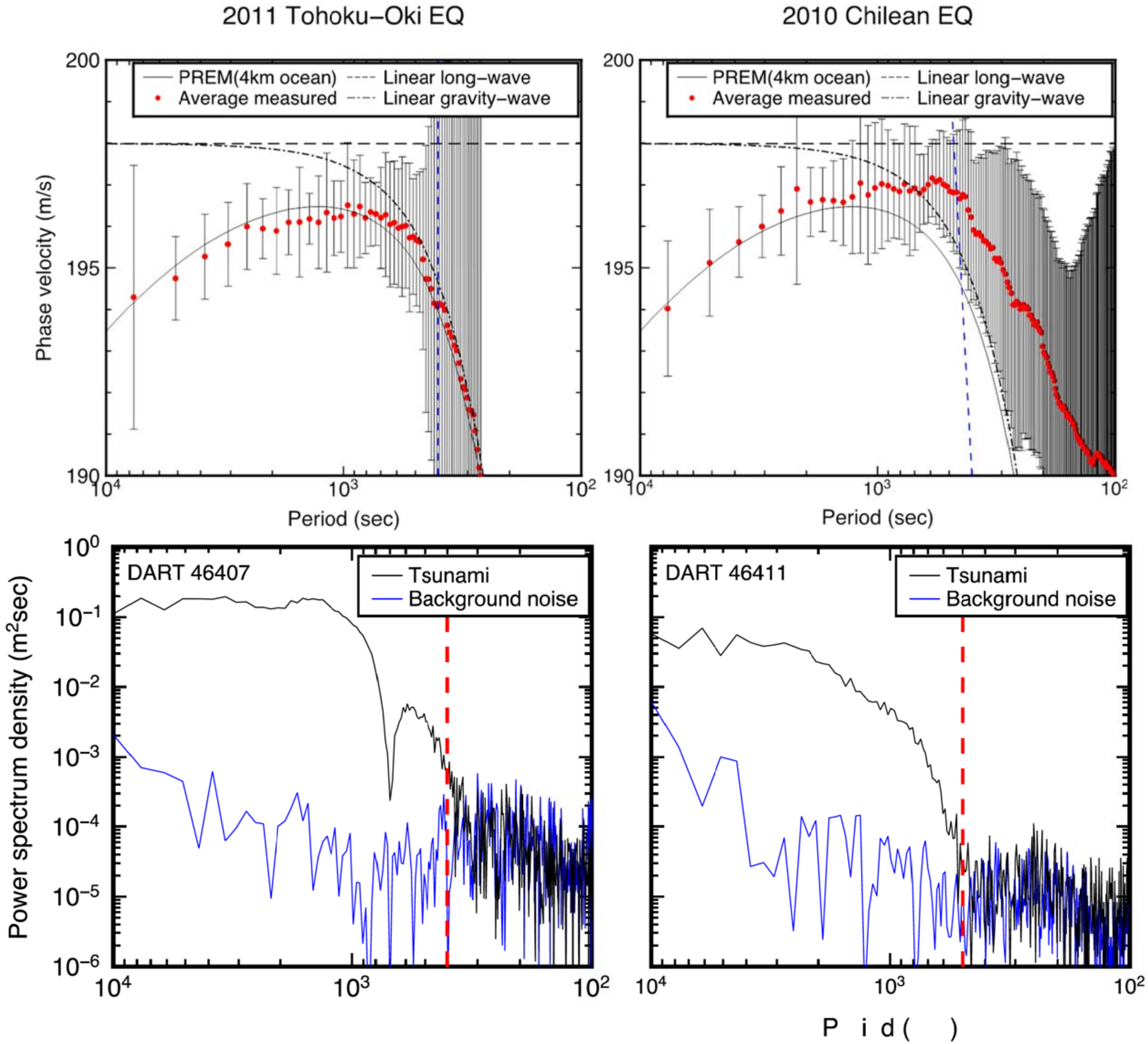

2011 Tohoku–Oki EQ
2010 Chilean EQ
PREM(4km ocean)
Average measured
Linear long–wave
Linear gravity–wave
Phase velocity (m/s)
Period (sec)
DART 46407
DART 46411
Tsunami
Background noise
Power spectrum density (m²sec)

2014 northern Chile EQ (M8.1) tsunami

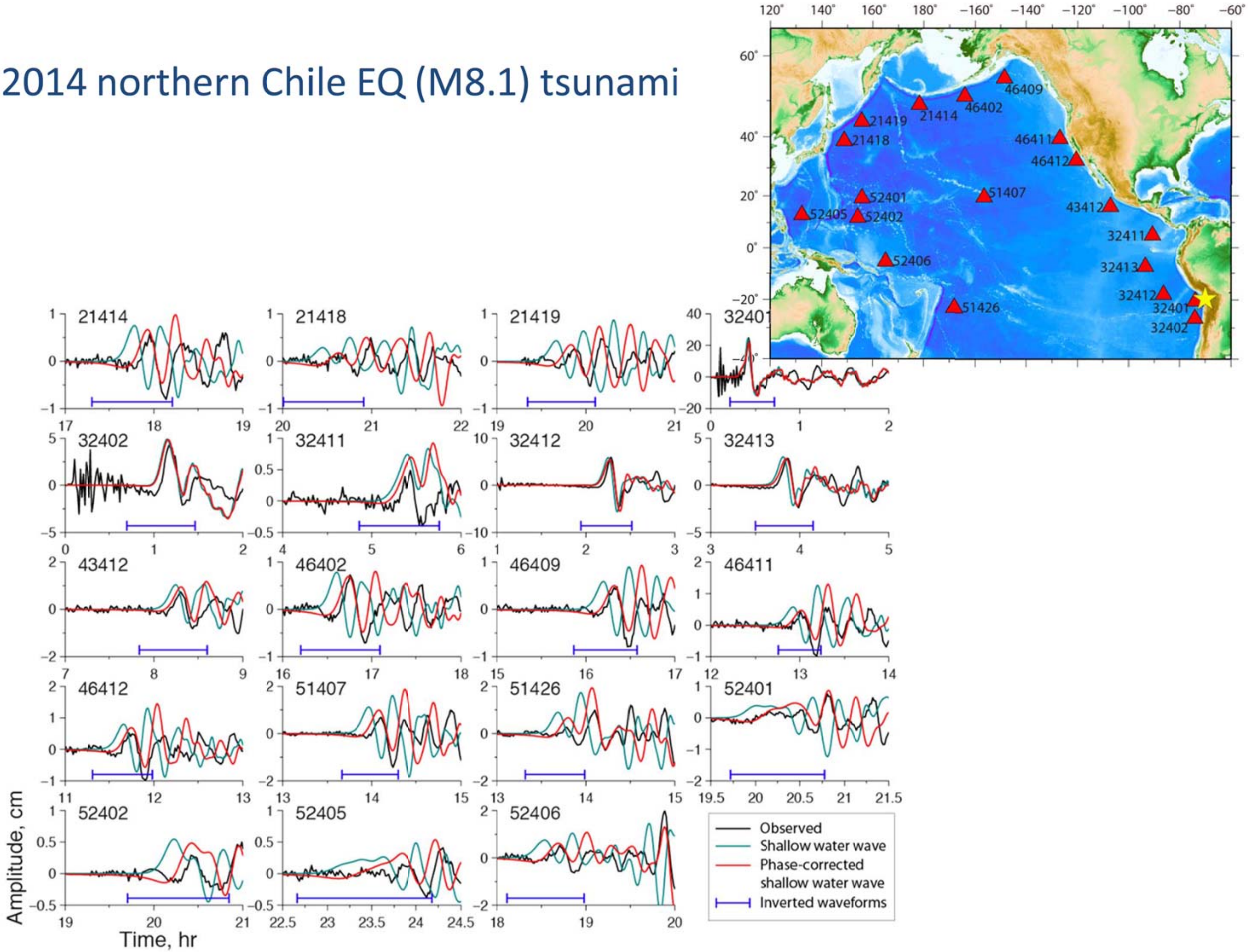

Traveltime delay of 2014 northern Chile tsunami

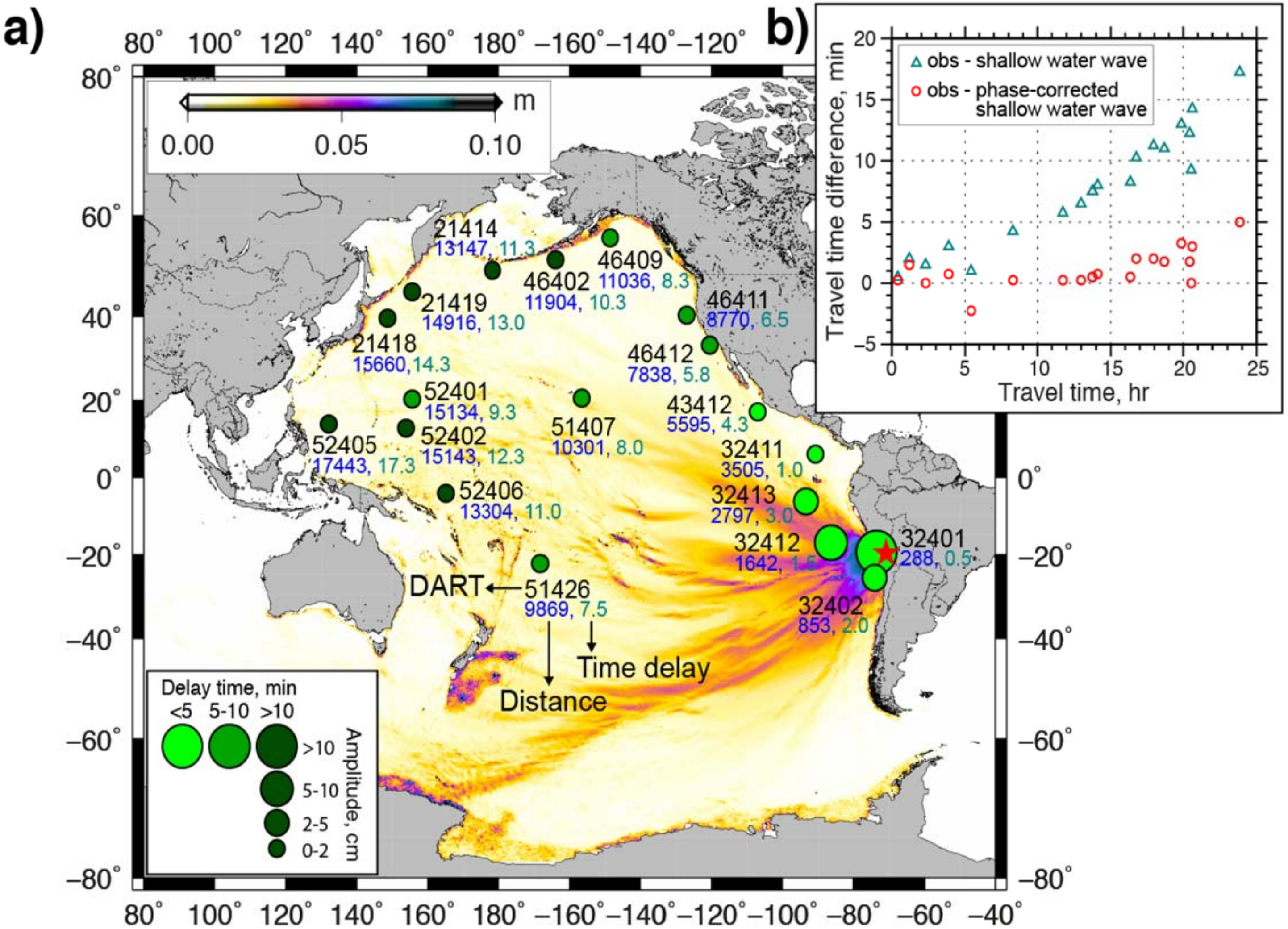

結論

- 遠地津波の遅延と初動反転は、太平洋を横断する津波（2010年チリ津波、2011年東北沖津波、2014年チリ津波）で共通して発生。

- これら遠地津波の特徴は、これまでの津波計算考慮してこなかった固体地球の弾性、海水圧縮性、海水移動に伴う地球重力場の変化の効果により生じた。

- これらの効果を含む簡便な津波計算方法（線形長波の位相補正）で、遠地津波波形をほぼ完全に説明可能。

- 2010チリ津波では、地震発生から１０時間以内の4箇所のDART観測点波形を利用して、日本沖合の津波（波高と時刻）を予測する断層モデル構築が可能。(2014年秋期地震学会、吉本他）

今後の対策

- 2010年チリ津波では日本の沖合（海底ケーブル、水深1500m）で
15分程度の到達遅延予測だが、日本沿岸（水深10m）では
30分程度の到達遅延が観測されている。

  →沖合の津波波形予測から沿岸の津波（波高と時刻）は説明可能か？

- 実際の遠地津波発生時に、リアルタイムで日本付近の津波（波高と時刻）
を予測できる津波波源モデルが構築可能か？

- 今回の遠地津波計算手法は津波の先頭部分（3時間程度）に適応可能。
海岸や海底地形で反射して到達する、津波後続波の予測には使えない。

  →後続波予測には、これらの効果に加え、津波の反射計算の
  高度化が必要。

参考文献

- Watada, S., and H. Kanamori, 2010, Acoustic resonant oscillations between the atmosphere and the solid earth during the 1991 Mt. Pinatubo eruption, J. Geophys. Res., 115, B12319, doi:10.1029/2010JB007747.

- Watada, S., S. Kusumoto, and K. Satake, 2014, Traveltime delay and initial phase reversal of distant tsunamis coupled with the self-gravitating elastic Earth, J. Geophys. Res., Solid Earth, 119, 4287–4310, doi:10.1002/2013JB010841.

- Gusman, A., S. Murotani, K. Satake, M. Heidarzadeh, S. Watada, E. Gunawa, and B. Schurr, 2014, Comparative evaluation of tsunami-GPS and teleseismic body wave inversion methods for the 2014 Iquique Chile earthquake, A21-12, Seism. Soc. J. fall meeting.

- 吉本昌弘・綿田辰吾・藤井雄士郎・佐竹健治, 2014, 遠方DARTを含む津波波形インバージョンから推定される2010年チリ地震（Mw8.8）の津波波源, S17-P07, 地震学会秋季大会.